Available online at www.sciencedirect.com
ScienceDirect
Acta Materialia 55 (2007) 3169–3175
Acta MATERIALIA
www.elsevier.com/locate/actamat

Atomistic investigation of the effects of temperature and surface roughness on diffusion bonding between Cu and Al

Shangda Chen [a,b,*], Fujiu Ke [a,b], Min Zhou [c], Yilong Bai [b]

[a] Department of Physics, Beihang University, Beijing 100083, China
[b] State Key Laboratory of Non-linear Mechanics (LNM), Institute of Mechanics, Chinese Academy of Sciences, Beijing 100080, China
[c] The George W. Woodruff School of Mechanical Engineering, Georgia Institute of Technology, Atlanta, GA 30332-0405, USA

Received 10 June 2006; received in revised form 28 December 2006; accepted 29 December 2006
Available online 7 March 2007

Abstract

Molecular dynamics (MD) simulations are carried out to analyze the diffusion bonding at Cu/Al interfaces. The results indicate that the thickness of the interfacial layer is temperature-dependent, with higher temperatures yielding larger thicknesses. At temperatures below 750 K, the interface thickness is found to increase in a stepwise manner as a function of time. At temperatures above 750 K, the thickness increases rapidly and smoothly. When surface roughness is present, the bonding process consists of three stages. In the first stage, surfaces deform under stress, resulting in increased contact areas. The second stage involves significant plastic deformation at the interface as temperature increases, resulting in the disappearance of interstices and full contact of the surface pair. The last stage entails the diffusion of atoms under constant temperature. The bonded specimens show tensile strengths reaching 88% of the ideal Cu/Al contact strength.

Keywords: Diffusion bonding; Molecular dynamics; Temperature effect; Tensile strength

1. Introduction

Diffusion bonding is a solid-state welding process that allows contacting surfaces to be joined under pressure and at elevated temperatures with minimum macroscopic deformation [1]. Almost all materials with compatible chemical and metallurgical properties can be diffusion-bonded [2]. This welding process has an inherent advantage over conventional welding since it does not involve the formation of unexpected phases at the bond interface which can occur in some advanced materials [2–6]. Theoretical and experimental studies have been carried out on diffusion bonding, primarily at continuum scales [1–8]. In contrast, analyses at atomic scale have scarcely been carried out. Molecular dynamics (MD) simulations has become one of the most widely used tools in nanomechanics primarily because it is not limited by uncertainties in sample preparation and test condition and can be used to analyzed a range of issues concerning mechanical behavior at the nanoscale. Weissmann et al. [9] used MD simulations to show that interfacial amorphization clearly develops at higher temperatures in a Co–Zr system. Chen et al. [10] calculated the interfacial energy of an face-centered cubic (fcc)/body-centered cubic interface in Ni–Cr alloys. Cherne et al. [11] investigated the amorphization of an Ni–Zr system. The microstructures of a Cu/Ta interface [12] and an SiO_2/Si interface [13] have also been analyzed by means of MD simulations. The conditions analyzed in these papers are significantly different from the conditions of actual diffusion bonding processes which involve combined high temperature and high pressure. As a result, interfacial diffusion does not occur and no transition regions are seen. Since temperature and pressure play an important roles,

* Corresponding author. Address: State Key Laboratory of Non-linear Mechanics (LNM), Institute of Mechanics, Chinese Academy of Sciences, Beijing 100080, China.
E-mail address: chensd@lnm.imech.ac.cn (S. Chen).

1359-6454/$30.00
doi:10.1016/j.actamat.2006.12.040

MD simulations accounting for such conditions can provide significant insight which may not be obtainable by other means. Another factor motivating MD analyses of diffusion bonding processes is the lack of quantification of the effects of surface roughness, which also plays an important role. MD simulations also offer the advantage of extensive parametric studies, potentially avoiding the need of long and expensive experiments. Recently, Chen et al. [14] reported an MD study of the pressure effect in diffusion bonding between Cu and Ag, and Liu et al. [15] investigated the cooling effect in diffusion bonding between Cu and Al. In the present paper, we consider the coupled temperature-roughness effects in the diffusion bonding of a Cu–Al material pair.

2. Simulation procedure

Interatomic potentials play a very important role in MD simulations. Considerable progress has been made in the development of empirical and semi-empirical many-body potentials. Well-established embedded atomic method (EAM) potentials [16] have been successfully used in analyzing elastic properties, defect formation energy and fracture mechanisms of various close-packed bulk metals. Here, the modified EAM model developed by Johnson [17,18] for alloys is adopted. This potential predicts heats of solution for the materials involved that is consistent with what is measured from experiments.

As shown in Fig. 1, the system analyzed consists of a monocrystal copper slab (top) and a monocrystal aluminum slab (bottom). The contact surfaces of Cu and Al are both (100) planes. The total numbers of the Cu and Al atoms in the model are 52,488 and 46,080, respectively. A parallel algorithm is used. Periodic boundary conditions are implemented in the two transverse directions. Three layers of atoms at the bottom of the Al slab and two layers at the top of the Cu slab serve as boundary atoms for the purpose of load or displacement application. The initial thermal velocities of atoms are assumed to follow the Maxwellian distribution. The Newton's equation of motion for the atoms is numerically integrated using the leap-frog algorithm [19] with a fixed time step of 2 fs. The external transverse pressure is maintained at atmospheric level, while the vertical pressure is 20 MPa. The structures are first equilibrated at 1 K for 10 ps and then heated up to a desired temperature (up to 750 K) at a rate of 5×10^{13} K s^{-1}. Subsequently, the temperature is kept constant at the desired value through the scaling of atomic momenta. To achieve sufficient interfacial diffusion, all calculations are carried out for 600 ps at the desired temperature.

3. Results and discussions

3.1. Effect of temperature

Atoms on either side of the interface can diffuse into the opposite side only if temperature is sufficiently high. Necessary levels of temperatures are usually between 0.6–0.8 T_m (where T_m represents the melting points of the materials involved). Since the melting point of Al is 933 K and that for Cu is 1083 K, the temperature levels of 600, 650, 700 and 750 K are considered here.

Fig. 1 shows the configuration of a cross-section of the structure after 600 ps of diffusion at different temperatures. At 600 K, only a small number of Cu atoms have diffused into the Al side and there is no obvious structural change since both sides retain their initial fcc lattice structures (see Fig. 1a). At 650 K (Fig. 1b), more Cu atoms have diffused into the Al side. When the temperature is higher than 650 K, more significant diffusion of Cu atoms into Al is seen, forming an Al-rich interfacial region. This interfacial region and the rest of the Al block exhibit an amorphous structural order when the temperature is at or above 650 K (Fig. 1b–d). This observation agrees well with the observation by Weissmann et al. [9] of a similar disordered interface in a Co–Zr system at high temperatures. Fig. 1 also shows that the diffusion is primarily one way, from the Cu side into the Al side. This is because Cu atoms have a smaller radius (2.556 Å) than that of Al atoms (2.886 Å). Obviously, it is easier for smaller atoms to diffuse into a region of larger atoms [20]. On the other hand, the melting

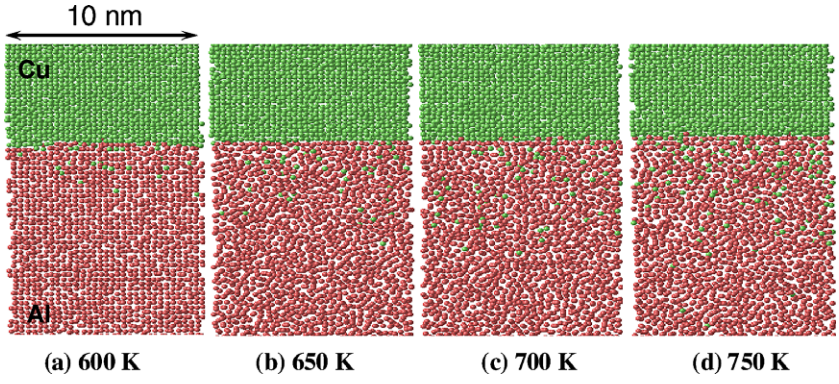

Fig. 1. Configurations of a cross-section at (a) 600 K, (b) 650 K, (c) 700 K and (d) 750 K after 600 ps. Only atoms near the interface are shown. Cu atoms are green and Al atoms are red. (For interpretation of the references to colour in this figure legend, the reader is referred to the conversion of this article.)

point of Cu is higher than that of Al, making it harder to break the bonds between Cu atoms than those between Al atoms, making it more difficult for Al atoms to diffuse into the Cu lattice. In contrast, the bonds in Al are weaker and vacancies form more easily. All three factors favor the diffusion of Cu atoms into Al, and not the other way around.

Fig. 2 shows the concentrations of Cu and Al atoms along the vertical direction for the four cases in Fig. 1. The region spanning both sides of the interface where the concentration of the solute atoms is over 5% is defined as the interfacial region. The size of this region can be determined from the concentration profiles. At 600 K, the thickness is approximately 6 Å (Fig. 2a), indicating very little diffusion across the interface. The thickness increases as temperature increases, with the values being 11, 19 and 30 Å at 650, 700 and 750 K, respectively.

Fig. 3 shows the thickness of the interfacial region as a function of time at different temperatures. At 600 K, the thickness fluctuates between 0 and 4 Å (smaller than two atomic layers) in the initial stage. After about 400 ps, the thickness reaches approximately 6 Å and does not show further increase except for minor fluctuations. At 650 K, the thickness shows stepwise increases to 11 Å by about 550 ps and shows no further increase thereafter. The profile for 700 K is similar to that for 650 K, except that the maximum thickness value is higher (18 Å). At 750 K, the thickness increases rapidly and continuously without saturation over the duration of the calculation.

3.2. Effect of surface roughness

Experiments have shown that the roughness of contact surfaces has a significant impact on the bonding process [21]. Some theoretical analyses have been carried out to address this issue at continuum scales [22–24]. In this section, we consider three different cases at the atomic scale:

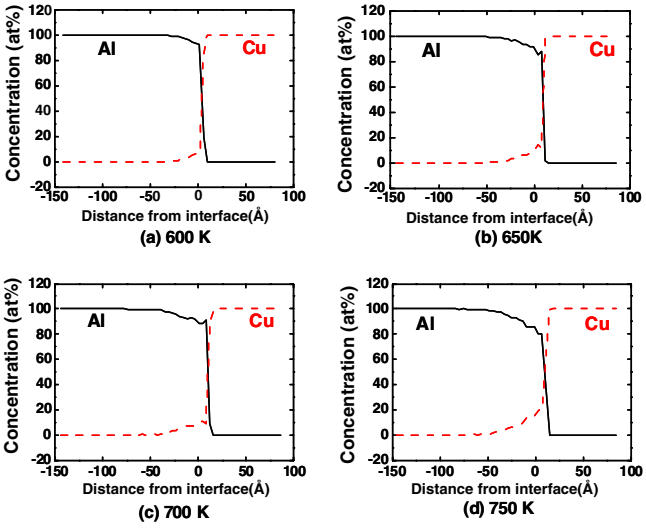

Fig. 2. Concentrations of Cu and Al atoms along the vertical direction at (a) 600 K, (b) 650 K, (c) 700 K and (d) 750 K after 600 ps.

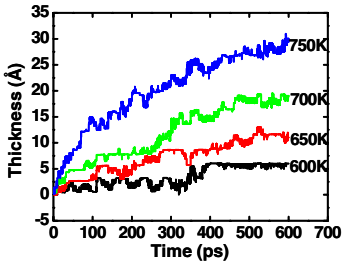

Fig. 3. Thickness of the interfacial region as a function of time at different temperatures.

(i) smooth Cu surface and rough Al surface with two protuberances of a height of 4 lattice constants for Al;
(ii) smooth Al surface and rough Cu surface with two protuberances of a height of 4 lattice constants for Cu; and
(iii) both surfaces are rough. In all three cases, the highest temperature is 700 K and the applied stress in the z direction is 20 MPa.

Fig. 4 shows the configurations of a cross-section at different temperatures for case (i). Obviously, the protuberances on the Al surface undergo significant deformation under stress, even at 200 K (Fig. 4b). However, interstices remain between the two sides. At 300 K, the protuberances are completely flattened and fully intimate contact is achieved. It should be noted that the heights of the protuberances in the simulations here are 1–2 orders of magnitude lower than those found in many laboratory diffusion bonding processes. This translates into a very large number of interstices between the surfaces at the macroscopic scale that is analyzed in Refs. [21,22]. Because Al is softer than Cu, more pronounced deformation is seen in Al. From Fig. 4c, it can also be seen that a layer of Al close to the interface becomes amorphous. The picture at 700 K is similar to that at 300 K, with no obvious diffusion of atoms across the interface in either direction.

Fig. 5 shows the same cross-section for case (ii). The smooth Al surface undergoes significant deformation under the applied stress when the temperature is increased to 200 K. Some of the Al atoms fill in the interspaces of the Cu surface (Fig. 5b). This process intensifies as temperature increases (Fig. 5c). At 400 K, the interspaces on the Cu surface are fully filled. The image at 700 is similar to that at 400 K, with no obvious diffusion between the two sides.

Fig. 6 shows the results for case (iii). The tops of the Al protuberances are flattened by the applied stress even before the temperature is increased. At 200 K, the Al side shows significant deformation, similar to that seen in previous cases. Some Al atoms fill in the interspaces of the Cu surface (Fig. 6b) and the protuberances on the Cu side show slight deformation. As the temperature increases, more Al atoms move into interspaces on the Cu surface (Fig. 6c). At 400 K, the interspaces are completely filled.

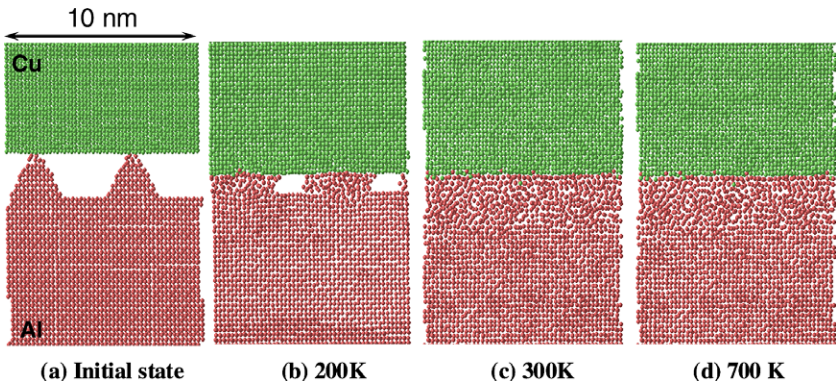

Fig. 4. Deformed configurations of a cross-section at different temperatures for case (i) (the stress is kept at 20 MPa).

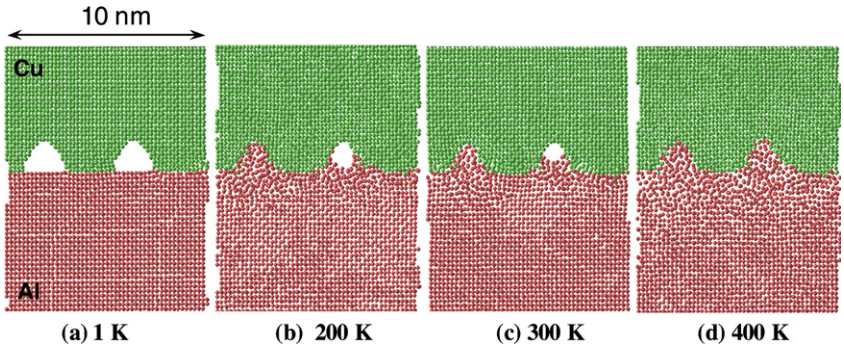

Fig. 5. Deformed configurations of a cross-section at different temperatures during heating for case (ii) (the stress is kept at 20 MPa).

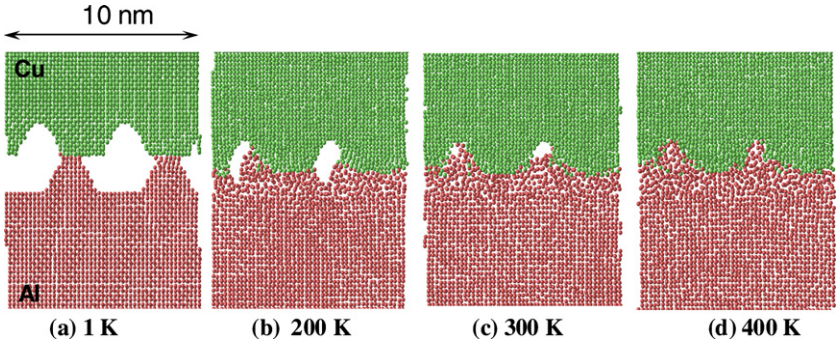

Fig. 6. Deformed configurations of a cross-section at different temperatures for case (iii) (the stress is kept at 20 MPa).

The results in Figs. 4–6 show that deformation primarily occurs in the Al, regardless of the configuration of the Cu surface. This is because Cu has greater strength and a higher melting point.

Fig. 7 shows the same cross-section as that in Figs. 4–6 after 600 ps at 700 K for cases (i) and (ii). As pointed out previously, the rough Al surface is flattened during heating before diffusion (Fig. 4d). Consequently, the diffusion pattern in Fig. 7a at 600 ps is similar to that in the case with perfectly smooth surfaces (Fig. 1). The diffusion pattern in Fig. 7b is very different from those in Figs. 1 and 7a. This difference arises because Al atoms have previously filled the interspaces during heating and the contact profile is similar to those in cases (ii) and (iii) when the Cu surface is rough before diffusion (Figs. 5d and 6d). Specifically, after 600 ps the contact profile is very similar to the initial profile of the Cu surface, except that it has become flatter (Fig. 7b).

The three sets of results show that the diffusion bonding process can be divided into three stages. In the first stage, the rough surface deforms under stress before heating, causing the contact area to increase. In the second stage, the softer (Al) surface undergoes significant deformation as temperature increases, causing the interstices to disappear and leading to fully intimate contact of the surfaces. The last stage is the diffusion of atoms at constant temperature. In Derby's theoretical model [22,23], possible diffusion bonding mechanisms were identified as: (i) plastic deformation of surface asperities; (ii) power-law creep deformation of the surface; (iii) diffusion of matter from interfacial void surfaces to growing necks; and (iv) diffu-

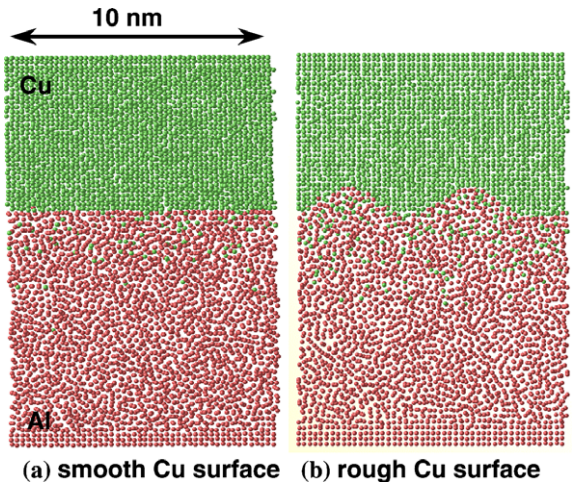

Fig. 7. Configurations of a cross-section after 600 ps at 700 K; (a) case (i), (b) case (ii).

sion of matter from bonded regions on the interface to growing necks. The MD results obtained here present a very similar understanding and therefore add credence to the continuum model. The only difference is that no interstices remain before diffusion in the MD simulations and therefore there is no diffusion of matter from interfacial voids to growing necks.

3.3. Tensile deformation

In order to examine and assess the mechanical properties of the diffusion-bonded Cu/Al samples, tensile loading is applied at 300 K to the diffusion-bonded Cu/Al pair in Fig. 1d which is obtained by bringing a perfect fcc Cu crystal and a perfect fcc Al crystal into contact and then allowing the structure to first equilibrate at 1 K for 10 ps, be heated up to 750 K at a rate of 5×10^{13} K s^{-1}, equilibrate at 750 K for 600 ps, and finally be cooled down to 300 K at a rate of 5×10^{13} K s^{-1}. For comparison purposes, the same tensile loading is also applied to monocrystal Cu, monocrystal Al, and a Cu/Al pair with ideal contact (obtained by bringing a perfect fcc Cu crystal and a perfect fcc Al crystal into contact and then allowing the structure to equilibrate at 300 K for 10 ps under atmospheric pressure). To effect the tensile deformation, the displacement of the boundary atoms is controlled by time steps. Each loading increment corresponds to a strain of 0.25% and is followed by a period of 8 ps of equilibration at constant strain. Although the strain rate for a loading step alone is approximately 3×10^{8} s^{-1}, which is several orders of magnitude higher than the rate in a typical tensile test, the equilibration periods following the load steps allow a steady state to be reached at the end of each increment. Therefore, the calculation here can be regarded as approximating quasistatic loading, as shown in a previous investigation [25].

Fig. 8 shows the nominal stress–strain curves for monocrystal Cu and Al, Cu/Al pair with ideal contact and diffusion-bonded Cu/Al pair. It can be seen that the stress reaches a maximum of 7.2 GPa at a strain of 11.5% for monocrystal Cu. Beyond the strain of 11.5%, the stress drops precipitously to 2.5 GPa and plastic flow occurs at stresses of around 2.5 GPa. The curve for monocrystal Al has features similar to those for monocrystal Cu, with a maximum stress of 4.9 GPa at a strain of 19.5%. When the strain exceeds 19.5%, the stress drops precipitously to 0.8 GPa and plastic flow occurs at stresses around 1 GPa. The curve for the ideal-contact Cu/Al pair is different from those for monocrystal Cu and Al. A sudden drop of stress appears first when the strain reaches 8.5%, followed by a second drop at a strain of 13%. The stress reaches a maximum of 3.6 GPa at a strain of 16%. When the strain is over 16%, stress drops from 3.6 to 1.6 GPa and the sample shows plastic flow. The flow stress is about 2 GPa. Finally, the case of the diffusion-bonded Cu/Al pair is similar to that of the ideal-contact Cu/Al pair, with no obvious sudden stress drop as strain increases. The stress–strain curve is flatter than that of the ideal-contact case. When the strain is over 6.5%, the stress shows a small drop and then increases as strain increases. The curve yields a tensile strength of 3.2 GPa, which occurs at a strain of 10.5%. The diffusion-bonded Cu/Al pair is quite strong, demonstrating a tensile strength that can reach 88% of that for the ideal-contact Cu/Al case. The stress drops from 3.2 to 1.5 GPa as the strain increases from 10.5 to 15%, and the increase from 15% to 22.5% is very gradual due to the plastic flow.

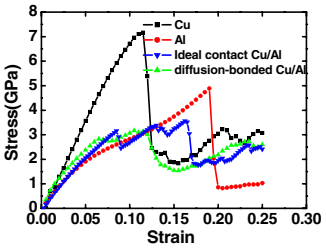

Fig. 8. Tensile stress–strain curves of monocrystal Cu and Al, Cu/Al pair with ideal contact and diffusion-bonded Cu/Al pair.

We now turn our attention to the deformed structures inside the samples to gain a better insight into the observed mechanical behaviors. Fig. 9 shows the deformed configurations of monocrystal Cu at different strains. Atoms with normalized centrosymmetry values between 0.88 and 0.92 are colored red. These atoms are associated with dislocations. Other atoms not involved in defects are colored blue. No obvious change in structure is observed as the strain increases from 0% to 11.5%, except for the elongation of the sample. The picture becomes very different at a strain of 12%, when many slip bands (red atoms) appear on the side surfaces. The slip bands on the surfaces form an angle of 45° relative to the loading axis (Fig. 9c and d). The formation of these slip bands results in the sudden drops of stress in the stress–strain curves discussed earlier. As the strain increases, more bands appear (Fig. 9d). The

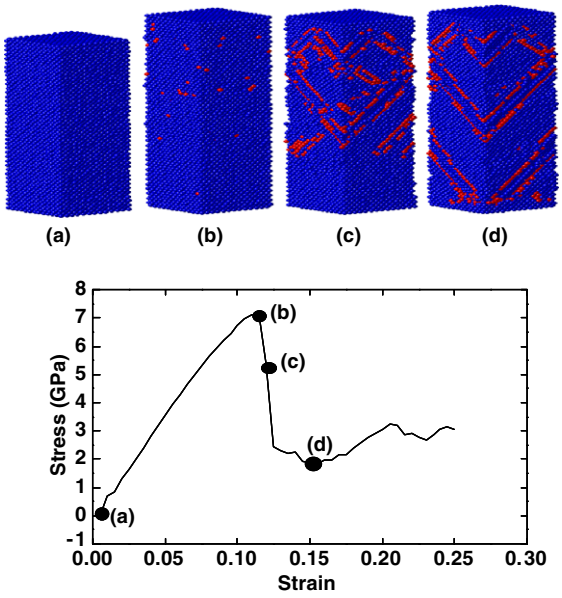

Fig. 9. Deformed configurations of monocrystal Cu at different levels of stain. Atoms with normalized centrosymmetry values between 0.88 and 0.92 are colored red, other atoms are blue. (For interpretation of the references to colour in this figure legend, the reader is referred to the conversion of this article.)

deformation of monocrystal Al is very similar to that of monocrystal Cu, except that slips bands begin to appear at a strain of 19% instead of 12%.

Fig. 10 shows deformed configurations of the ideal-contact Cu/Al pair at different strains. In Fig. 10-(1), or the top row of images, Cu atoms are blue and Al atoms are red. In Fig. 10-(2), or the second row of images, only atoms with normalized centrosymmetry values between 0.86 and 0.92 are shown. Fig. 10a and b shows that there is no obvious dislocation activity in Cu before a strain of 8.5%; however, active dislocations are seen in the Al half (Fig. 10-(2)a and b). At a strain of 9%, a few slip bands appear on the side surfaces on the Al side and an Al layer adjacent to Cu becomes amorphous (Fig. 10-(1)b, not shown clearly). The appearance of slip bands on the Al side results in the sudden drop of stress at a strain of 8.5%. Some of the slip bands disappear and new slip bands appear as strain increases (Fig. 10-(1)b and c). From Fig. 10-(2)b and c, it can be seen that some dislocations in the Al half disappear as strain increases. This process is accompanied by the emergence of dislocations in the Cu half. At strains above 16% (Fig. 10d), slip bands appear on the Cu side (not shown clearly), resulting in another sudden drop in stress. Further deformation is associated primarily with the development of additional slip bands on the Cu side (not shown).

Fig. 11 shows deformed configurations of the diffusion-bonded Cu/Al pair at different strains. The results are similar to those for the ideal-contact case in the following ways. First, there are no obvious changes in Cu before a strain of 7% (Fig. 11-(1)a); however, some dislocations are seen in the Al half (Fig. 10-(2)a). The dislocations move to the Al surface (Fig. 10-(2)b), appearing as slip bands on the side surfaces. This process also involves the amorphization of a layer of Al immediately next to the interface (Fig. 11-(2)b, not clearly shown). The appearance of slip

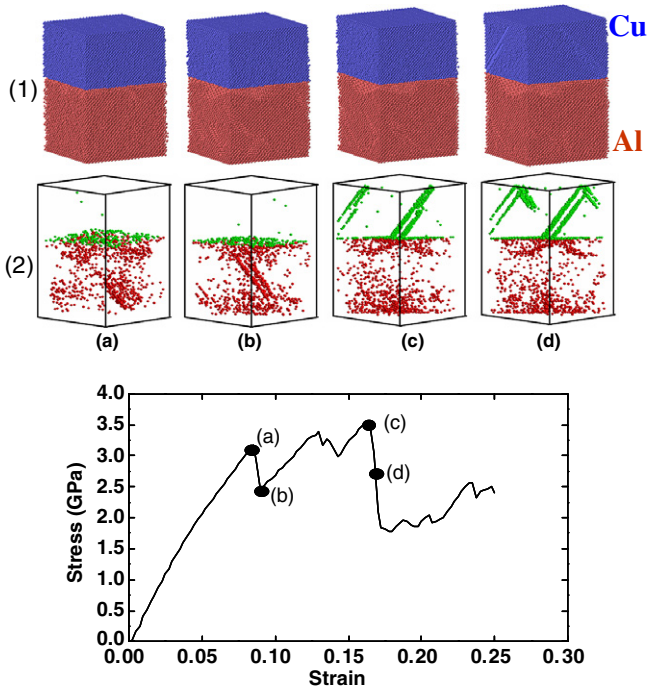

Fig. 10. Deformed configurations of ideal-contact Cu/Al pair at different strain levels: (a) 8.5%, (b) 9%, (c) 16% and (d) 16.5%. Only atoms with normalized centrosymmetry values between 0.86 and 0.92 are shown in (2).

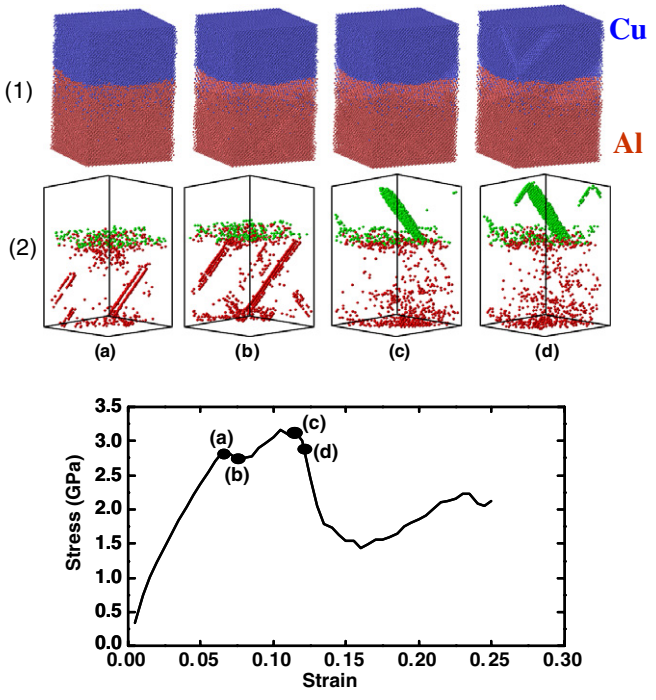

Fig. 11. Deformed configurations of diffusion-bonded Cu/Al pair at different strain levels: (a) 6.5%, (b) 7% , (c) 10.5% and (d) 11%. Only atoms with normalized centrosymmetry values between 0.86 and 0.92 are shown in (2).

bands on the Al side and the amorphization cause the stress to decrease slightly, beginning at a strain of 6.5%. The dislocations in Al do not propagate through the interface (Fig. 11-(2)b and c). Further deformation is associated with the disappearance of dislocations on the Al side and the emergence of dislocations on the Cu side (Fig. 11-(2)c and d). Phenomenologically, this leads to strain hardening, as seen in the stress–strain relation. When the strain is over 10.5%, dislocations reach the side surface of the Cu half (Fig. 11-(2)d) and slip bands appear (Fig. 11-(1)d, not clearly visible), resulting in the second drop of stress.

To summarize, the stress–strain curves show that the tensile strengths of monocrystal Cu, monocrystal Al, ideal-contact Cu/Al and diffusion-bonded Cu/Al are, respectively, 7.2, 4.9, 3.6 and 3.2 GPa. These strength values demonstrate the effectiveness of the diffusion bonding process in creating a bond between the two metals. The strength values here are one order of magnitude higher than those from experiments [26], primarily because the material models contain no initial defects, such as dislocations, voids, grain boundaries and impurities.

4. Conclusions

MD simulations of the Cu/Al diffusion bonding process and the subsequent tension deformation have been carried out. The primary findings are:

(1) Temperature plays a very important role in the bonding process. When the temperature is lower than 600 K, no obvious diffusion occurs. Above 600 K, higher temperatures yield thicker interfacial layers. The thickness of the interfacial region increases in a stepwise manner when the temperature is lower than 750 K and increases rapidly and continuously when temperature is higher than 750 K.
(2) When surface roughness is present, the bonding process can be divided into three stages. In the first stage, the rough surface deforms under stress before heating, resulting in an increase in contact area. In the second stage, the surface deforms significantly as temperature increases. Also, interstices disappear and fully intimate contact is achieved in this stage. The last stage entails diffusion of atoms.
(3) The diffusion-bonded Cu/Al surface pair obtained under the conditions analyzed demonstrates very good mechanical properties, with a tensile strength of about 88% of that of the ideal contact Cu/Al pair. The deformation mechanism of diffusion-bonded Cu/Al interfaces is not the same as those for single crystal Cu and Al. The interface between the dissimilar materials blocks the propagation of dislocations from the Al region into the Cu region, giving rise to more pronounced strain hardening when compared with the monocrystals.

Acknowledgements

This research is supported by the National Natural Science Foundation of China through Grant nos. 10372012, 10432050 and 10528205. The computations are performed on the PC clusters of the State Key Laboratory for Scientific and Engineering Computing of the Chinese Academy of Sciences.

References

[1] Owczarski WA, Paulonis DF. Weld J 1981;62:22.
[2] Guo ZX, Ridley N. Mater Sci Technol 1987;3(11):945.
[3] Fukumoto S, Hirose A, Kobayashi K. Prod Eng 1989;46:374.
[4] Aleman B, Gutierrez I. Trans A 1995;26(2):437.
[5] Aleman B, Guterrez I, Urcola JJ. Scripta Mater 1997;36(5):509.
[6] Askeland DR. The science and engineer of materials. Hong Kong: Van Nostrand Reinhold; 1989.
[7] Yilmaz O, Celik H. J Mater Process Technol 2003;141:67.
[8] Wang A, Ohashi O, Norio Y, et al. J Electron Microsc 2004;53(2):157.
[9] Weissmann M, Ramfrez R, Kiwi M. Phys Rev B 1992;46:2577.
[10] Chen JK, Frakas D, Reynolds WT. Acta Mater 1997;45:4415.
[11] Cherne FJ, Baskes MS, Schwarz RB. J Non-crystal Solids 2003;317:45.
[12] Heino P. Comput Mater Sci 2001;20:157.
[13] Watanabe T, Tatsummura K, Ohdomari I. Appl Surf Sci 2004;237(1–4):125.
[14] Chen SD, Soh AK, Ke FJ. Scripta Mater 2005;52:1135.
[15] Liu H, Ke FJ, Pan H, et al. Acta Physica Sinica 2007;56(1):407 [in Chinese].
[16] Foiles SM, Baskes MI, Daw MS. Phys Rev B 1986;33(12):7983.
[17] Johnson RA. Phys Rev B 1989;39:12554.
[18] Zhou XW, Wadley HNG, Johnson RA, et al. Acta Mater 2001;49:4005.
[19] Hockney RW. Methods Comput Phys 1970;9:136.
[20] Richmond O, Morrison HL, Devenpeck ML. Int J Mech Sci 1974;16(1):75.
[21] Zuruzi AS, Li H, Dong G. Mater Sci Eng A 1999;270:244.
[22] Derby B, Wallach ER. Metal Sci 1982;16:49.
[23] Derby B, Wallach ER. Metal Sci 1984;18:427.
[24] Elzey DM, Wadley HNG. Acta Metall Mater 1993;41(8):2297.
[25] Xu Z, Liang HY, Wang XX. Acta Mech Solida Sin 2003;24(2):229.
[26] Shen YF, Lu L, Lu QH, et al. Scripta Mater 2005;52(10):989.